GABAergic circuits control stimulus-instructed receptive field development in the optic tectum

Blake Aaron Richards, Oliver Paul Voss, Colin Jon Akerman

GABAergic circuits control stimulus-instructed receptive field development in the optic tectum

Blake A. Richards, Oliver P. Voss & Colin J. Akerman

Department of Pharmacology, Oxford University, Mansfield Road, Oxford, OX1 3QT, UK
Correspondence should be addressed to Colin Akerman (colin.akerman@pharm.ox.ac.uk)

Acknowledgements:
We would like to thank Holly Cline, Karri Lamsa and Ole Paulsen for helpful discussions and for comments on the manuscript. This work was supported by grants from the Biotechnology and Biological Sciences Research Council (BB/E0154761) and the Medical Research Council (G0601503). The research leading to these results has received funding from the European Research Council under the European Community's Seventh Framework Programme (FP7/2007-2013), ERC grant agreement No. 243273. In addition, CJA was supported by a Fellowship from the Research Councils UK and British Pharmacological Society, and BAR was supported by a Wellcome Trust Doctoral Fellowship and a Post Graduate Scholarship from the Natural Sciences and Engineering Research Council of Canada.

Authors contributions:
BAR conducted the experiments. BAR, OPV and CJA designed the experiments, contributed to the data analysis, preparation of the figures and wrote the manuscript.

Abstract

During the development of sensory systems receptive fields are modified by stimuli in the environment. This is thought to rely upon learning algorithms that are sensitive to correlations in spike-timing between cells, but how developing circuits selectively exploit correlations that are related to sensory inputs is unknown. We explore this by recording from neurons in the developing optic tectum of *Xenopus laevis*. We report that repeated presentation of moving visual stimuli induces receptive field changes that reflect the properties of the stimuli and that this form of learning is disrupted when GABAergic transmission is blocked. Consistent with a role for spike-timing dependent mechanisms, GABA blockade alters spike-timing patterns in the tectum and increases correlations between cells that would impact plasticity at intratectal synapses. This is a previously unknown role for GABAergic signals in development and highlights the importance of regulating the statistics of spiking activity for learning.

The development of visual circuits involves a diverse array of endogenous and exogenous signals[1], including both spontaneous and environmentally driven neural activity[2]. Early seminal experiments illustrated the remarkable sensory driven plasticity of primary systems[3], and later studies suggested that activity is not just permissive but plays an instructive role in the formation of neural circuits[4,5]. These results have been expanded upon and it is now known that the content of the visual environment is reflected in the functional changes that activity induces[6-10]. Evidence suggests that neurons can learn about the spatiotemporal properties of the visual environment by utilizing temporally asymmetric Hebbian learning algorithms, such as spike-timing-dependent plasticity (STDP)[8,10-12]. Computational studies have also provided formal demonstrations that changes in receptive fields induced by these plasticity rules could underlie functional properties like direction selectivity[13,14]. The consequences of Hebbian learning depend on the specific correlations in spiking activity between cells[15], and it is not known how developing systems control the statistical properties of their activity to ensure that features in the environment are translated into functional properties. One possibility is that γ-amino-butyric acid (GABA) mediated signals provide this control by limiting correlations in activity between neurons of developing sensory systems[16].

In mature systems, GABAergic inhibition regulates the timing of activity by sharpening the temporal precision of spiking[17-19] and by generating synchronizing oscillations[20]. The role for GABA as a regulator of temporal activity patterns early in development is less clear in part because GABA-A receptor signaling can be quite different at these stages. Compared to mature systems, GABAergic transmission in a variety of developing systems has been shown to have different kinetics[21-23], greater input strengths relative to glutamatergic inputs [24-26], and a depolarizing effect on the membrane potential[21,27,28]. An open question, therefore, is exactly how

immature GABAergic systems affect the spatiotemporal statistics of environmentally driven activity, and whether this is important for instructive learning.

Here, we report experiments conducted using *in vivo* recordings in the optic tectum of *Xenopus laevis* embryos during early stages of development. We show that tectal neurons can be "trained" by repeatedly presenting a visual stimulus and that the resulting changes induced in their receptive fields reflect the spatiotemporal properties of the training stimulus. In contrast, when GABAergic transmission in the tectum is blocked, receptive fields may change following a period of training but the instructive effects of the visual input are eliminated. This elimination of instructive learning may be related to changes in spike-timing patterns because when GABAergic inputs are blocked, there is a substantial increase in the spike-timing correlations between tectal cells and greater potential for tectal-tectal synaptic plasticity. Rather than decreasing the variance in spike-timing, as they do in some adults systems[17-20], early GABAergic circuits in the tectum enhance spatiotemporal differences in spiking and minimize correlations that may be introduced via recurrent excitation. This may provide a mechanism to ensure that receptive field changes are instructed by the statistics of the visual environment.

Results

Moving stimuli instruct asymmetric receptive field changes

Previous work in the optic tectum of *Xenopus laevis* tadpoles has demonstrated that moving stimuli can induce changes in the excitatory synaptic inputs to cells that are asymmetric with respect to the direction of movement[6,11]. As a first step towards understanding the potential role of GABA in instructive learning, we wanted to determine whether moving stimuli in the environment would produce similar changes in the receptive fields of tectal neurons as determined by their output (i.e. spiking activity) and under physiologically realistic conditions in intact cells (Fig. 1a).

Tectal neurons in tadpoles at stages 41-44 were loose-patched in cell-attached mode to enable monitoring of their spiking activity, without disruption of their internal milieu, and we mapped receptive fields by flashing white squares on a black background (Fig. 1b, left; Supplementary Fig. 1; see Methods). We restricted our analysis of receptive fields to the responses following the disappearance of the square[25], as these are much more robust in these early stages[29]. Training stimuli consisted of a white bar that drifted across a black screen in a randomly selected direction[6,11] (Fig. 1b, right). To assess the effects of the training we mapped the receptive fields both before and after training in order to generate a 'pre-training' and a 'post-training' receptive field, respectively. We then subtracted the pre-training receptive field map from the post-training receptive field map and the resulting 'subtraction receptive field' depicted the training-induced changes at each location of the receptive field (Fig. 1c).

Cells varied in terms of the extent to which they exhibited receptive field changes following training, with an overall trend towards potentiation in spike rate of 23.9 ± 13.2 % (mean ± s.e.m.; n = 18 cells). However, there was a clear asymmetry in the receptive field changes, which was in

accordance with the direction of movement of the training stimulus (Fig 2a-e). These instructive effects were quantified by analyzing the subtraction receptive fields (see Methods). Changes in the receptive fields that were measured along the direction of movement of the training stimuli showed a pronounced asymmetry (Fig. 2a). The change in receptive field regions that were stimulated before the receptive field center was 10.1 ± 3.1 % above the average, while the changes in regions stimulated after the center was –7.2 ± 2.6 % below the average (Fig 2b, 'Early' vs. 'Late'). This asymmetry in the receptive field differences was highly significant (P = 0.0065, paired t-test). We also measured the angle of the direction from the post-training receptive field center to the pre-training receptive field center and found that this angle was significantly correlated with the direction of movement of the training stimulus (Fig. 2c; Pearson's r = 0.52, P = 0.035). When we examined changes along the direction orthogonal to the direction of training we did not observe any asymmetry (Fig. 2d). To verify that the differences we observed were a result of the training we also inspected "untrained" cells that were presented with a blank screen during the equivalent of the training period (n = 21 cells). Changes in these cells were small and topographically random, such that measurements across their subtraction receptive fields were flat and close to zero (Fig. 2e).

To compare the data we calculated an "asymmetry coefficient", which measured the difference across the subtracted receptive field map along a particular direction (see Methods). Trained cells showed asymmetry coefficients that were significantly different from zero in the direction of movement of the training stimuli, but not in the orthogonal direction (Fig. 2f, 'Trained' P = 0.0007, and 'Orth' P = 0.69, t-test). In cells where a second receptive field map was recorded 25 minutes after training, the asymmetry coefficients were still significantly different from zero (P = 0.038, t-test, n = 7 cells), and there was no significant difference

between the two post-training receptive fields (P = 0.8, paired t-test), indicating that the changes can be persistent. As expected, the asymmetry in the untrained cells was not significantly different from zero (Fig. 2f, 'Blank' P = 0.34, t-test), nor was it in two cells that had not spiked during the training (Fig. 2f, 'No spikes', P = 0.32, t-test).

GABA circuits control instructive receptive field changes

To determine whether GABAergic signaling within the tectum is important for these instructive receptive field changes, we repeated the training protocols but with local application of 50 μM SR-95531 ("gabazine") (Fig. 3a), which is a competitive GABA-A receptor antagonist (Supplementary Fig. 2). The mean change across the receptive field following training in SR-95531 was 47.5 ± 38.7 % (n = 19 cells), which was not significantly different to controls (P = 0.57, t-test), illustrating that GABAergic signals are not required for potentiation. However, unlike in the control condition, the instructive component of the differences was no longer apparent, and the changes in the receptive fields appeared to be random in their topography (Fig. 3a-d). The mean change in spiking activity was equivalent across the receptive field (Fig. 3b), and similar to the changes observed in the orthogonal direction (Fig. 3d). Equally, comparing the relative change between those areas stimulated before and after the pre-training center did not reveal any asymmetry, with either region equally likely to show greater potentiation than the other (Fig. 3c; 'Early' vs. 'Late', P = 0.5, paired t-test). GABA blockade also abolished the correlation between the angle of the direction of shift in the receptive field center and the direction of movement of the training stimuli (Pearson's r = –0.34, P = 0.23, n = 14; 5 cells showed zero movement in their centers). The asymmetry coefficients in the training direction were significantly higher for the control cells than cells trained under GABA blockade (Fig 3e; P

= 0.003, *t*-test). Also, the asymmetry coefficients for cells with GABA blockade were not significantly different from zero for the trained direction ('Train SR-9'; $P = 0.5$, *t*-test), the direction orthogonal to the training direction ('Orth.'; $P = 0.95$, *t*-test), or 0° direction when no training stimulus was presented ('Blank' $P = 0.78$, *t*-test, n = 9). The lack of asymmetric changes under GABA blockade was not a result of an inability to detect training-induced changes because the signal-to-noise ratio in the subtracted receptive fields was comparable between the two groups (Control signal-to-noise = 1.55 ± 0.16, SR-95531 signal-to-noise = 1.46 ± 0.21, $P = 0.74$, *t*-test). In summary, GABAergic signaling may not be necessary for some stimulus-induced changes to occur, however it is necessary if receptive field changes are to reflect the properties of the visual stimuli.

Next we examined whether the elimination of instructive learning during SR-95531 application could be linked to any changes in the receptive fields prior to training. In fact, the effects of GABA-A receptor blockade on untrained receptive field maps were relatively subtle (Fig. 4a). The mean rate of fire across the receptive fields (control = 2.4 ± 0.4 Hz, SR-95531 = 2.0 ± 0.4 Hz, $P = 0.42$, *t*-test), maximum rate of fire (control = 19.5 ± 3.0 Hz, SR-95531 = 17.0 ± 3.8 Hz, $P = 0.61$, *t*-test), receptive field size (control = 3,968 ± 670 degrees^2, SR-95531 = 3,683 ± 665 degrees^2, $P = 0.75$, *t*-test; see Methods) and spontaneous activity of the neurons (control = 1.0 Hz [95% C.I. = 0.5-1.0] (median with 95% confidence interval), SR-95531 = 0.6 Hz [95% C.I. = 0.2-1.0], $P = 0.36$, Mann-Whitney *U*-test), were all not significantly altered by the drug, suggesting that GABAergic signals in this system are not solely excitatory or solely inhibitory. The one significant difference was that in untrained cells SR-95531 altered the temporal distribution of spikes ($P = 1.0 \times 10^{-5}$, Kolmogorov-Smirnov test). Under GABA blockade the first spikes tended to occur later and all the spikes appeared over a narrower time window, when

compared to spikes recorded when GABAergic signaling was intact (Fig. 4b-c). This data suggested that the impact of SR-95531 on training-induced receptive field changes may relate to the effects of GABAergic signals on the temporal statistics of spiking activity in the tectum.

GABA signaling alters correlations in spike-timing

If the temporal statistics of spiking activity are altered under GABA blockade, this could impact synaptic plasticity mechanisms recruited during training. The overall number of spikes produced during training was not different under GABA blockade (control = 2.64 ± 0.42 spikes per presentation of the training stimulus, SR-95531 = 2.85 ± 0.71 spikes per presentation, $P = 0.81$, *t*-test). However, control cells showed much greater heterogeneity in the timing of their responses during training. Some control cells spiked relatively early during presentation of the bar stimulus, whereas other cells either spiked later or exhibited spiking throughout the period that the bar was presented (Fig. 5a). In contrast, the spiking behavior of the SR-95531 cells was much more homogenous such that these cells typically responded with bursts of action potentials at relatively early times during the presentation of the bar (Fig. 5b).

We were curious as to whether these changes affected the degree of correlation in spike-times between tectal cells, as this would be relevant for correlation based Hebbian plasticity mechanisms[15]. Pair-wise correlations between the spike-time histograms of cells showed that GABA blockade significantly increased the degree of tectal-tectal spike-timing correlations during the training protocol from 0.024 [95% C.I. = 0.013-0.035] to 0.045 [95% C.I. = 0.031-0.073] ($P = 0.0004$, Mann-Whitney *U*-test).

Receptive field changes are sensitive to spike-timing

If changes in spike-timing are responsible for the lack of instructive learning under GABA blockade then other manipulations that alter the temporal statistics of tectal spiking should also interfere with instructive learning. Moreover, different effects upon spike-timing should produce different changes to receptive fields. To test this we altered the relative balance of glutamatergic and GABAergic receptor activity during training by puffing glutamate onto the tectum and in a second experiment we interfered with spiking activity during training by direct electrical stimulation of the tectum.

When glutamate (L-glutamic acid, 10 mM) was puffed locally onto the tectum at the start of each presentation of the training stimulus (see Methods), the effect on tectal spike-times was the opposite of SR-95531 application. Tectal cells showed greater diversity in their spiking activity during training paired with glutamate puffs, presumably because the exogenous agonist strongly influenced the temporal profile of glutamate receptor activity (Fig. 6a, n = 9 cells). Importantly, the effect of this type of training upon receptive fields was also different to that observed under GABA-A receptor blockade, as training paired with glutamate puffs showed a tendency towards depression across the receptive field (mean change of –13.1 ± 7.1 %), with no evidence of instructive asymmetry (Fig. 6b-c and 6g).

Electrical stimulation of the tectum provided greater temporal control and therefore the opportunity to shift tectal spike-times in a way that resembled the effects of SR-95531. For each presentation of the training stimulus, electrical stimulation was timed to occur 200 ms following the onset of the visual stimulus, during the peak of the visually-evoked responses. The effects of training paired with electrical stimulation were qualitatively much more similar to the effects of GABA-A receptor blockade, both in terms of the spiking activity during training and the effects

of training upon receptive fields. During training paired with electrical stimulation the cells exhibited temporally synchronous, short bursts of action potentials, and therefore the population of spike times had a narrow distribution (Fig. 6d). Receptive field changes under these conditions showed strong potentiation (mean change of 142 ± 64.2 %) and a lack of instructive asymmetry (Fig. 6e-g).

These effects were not linked to overall spike count, as the number of spikes per presentation of the training stimulus was 2.58 ± 0.82 with glutamate puffs, and was 3.31 ± 0.78 with electrical stimulation, neither of which was significantly different from the control or SR-95531 conditions (Fig. 6h; $P = 0.88$, one-way ANOVA). However local application of glutamate during training produced a significant drop in the spike-timing correlations between tectal cells relative to the control condition, while electrical stimulation produced a significant increase (Fig. 6i; $P = 1.0 \times 10^{-5}$, Kruskal-Wallis one-way ANOVA).

These manipulations could affect receptive field changes via synaptic plasticity mechanisms that are sensitive to temporal correlations in spiking activity, such as STDP[11,30]. To investigate this we developed a Monte-Carlo simulation that used the spike-times recorded during presentation of the training stimuli and incorporated a STDP function that has been described in the tectum[30]. The simulation estimated the potential for tectal-tectal STDP, without distinguishing between long-term potentiation (LTP) or depression (LTD) (see Methods and Supplementary Fig. 3 for details). Interestingly, the groups were highly significantly different in their values for this STDP estimate ($P = 1.0 \times 10^{-5}$, Kruskal-Wallis one-way ANOVA), with cells in both the SR-95531 and electrical stimulation conditions showing a significant increase in their potential for STDP compared to control cells (Fig. 6j). The results from these experiments demonstrate that receptive field changes are highly sensitive to spike-timing during training, and

support the idea that GABAergic circuits regulate stimulus-induced instructive learning by modulating the temporal statistics of spiking.

GABAergic circuits reduce spatiotemporal correlations

Our examination of responses during receptive field training indicated that at these stages of *Xenopus* development, local GABAergic circuits function by reducing correlations in spike-times. To explore this aspect of GABAergic signaling more thoroughly we performed a more comprehensive spatiotemporal receptive field mapping paradigm (see Methods). The resulting maps revealed that control cells displayed substantial variety in their temporal response profiles for different locations in visual space (Fig. 7a). Individual cells were quite different from each other in terms of which stimulus locations triggered responses at different post-stimulus times. In contrast, pharmacological blockade of GABAergic signaling resulted in much more uniform temporal response profiles across visual space (Fig. 7b). On average, response profiles of pairs of control cells exhibited 'between-cell' correlations (see Methods) of only 0.1 [95% C.I. = 0.06-0.14], whereas the value for SR-95531 cells was 0.57 [95% C.I. = 0.43-0.65] and represented a highly significant difference (control n = 21 cells, SR-95531 n = 7 cells, $P = 1.0 \times 10^{-5}$, Mann-Whitney *U*-test).

The variety of responses under control conditions suggested that an individual cell would also show a low degree of correlation in its own responses across time. Indeed, we found that 'within-cell' correlations (see Methods) were low in the control condition, with an average of 0.04 ± 0.01 and this was significantly lower than those observed for SR-95531 cells, which showed an average within-cell correlation of 0.43 ± 0.09 ($P = 1.0 \times 10^{-5}$, *t*-test). This data

demonstrates that GABAergic signals in the developing tectum introduce diversity in spiking responses following stimulation of different locations in the visual field.

Timing of synaptic inputs may underlie learning

In mature systems feed-forward GABAergic inhibition can decrease variance in spike-timing by providing a limited temporal window during which early mono-synaptic excitation is able to trigger action potentials[17-19]. In young systems, including the optic tectum at the stages studied here, GABA is thought to exert a depolarizing influence on the membrane potential[21]. The effects of depolarizing GABAergic signals can be either excitatory[31] or provide a shunting inhibition of other depolarizing inputs[32]. This produces diverse inhibitory effects[33] that are dependent on the timing of GABAergic signals relative to glutamatergic inputs[34,35]. Regardless of its effect on the membrane potential, if GABAergic signals consistently followed glutamatergic signals with the same, short delay (e.g. via a disynaptic feed-forward GABAergic pathway), the GABAergic signals would be expected to *decrease* temporal diversity in spiking activity. Our observation that GABAergic signals actually *increase* temporal diversity in tectal spiking activity extends previous work[21,36] and invokes an expanded model of the immature optic tectum with diverse temporal relationships between glutamatergic and GABAergic inputs (Supplementary Fig. 4).

If this is correct then different regions of a tectal receptive field should exhibit different latencies in the onsets of glutamatergic and GABAergic synaptic inputs. To test this we recorded visually-evoked synaptic currents from tectal neurons in whole-cell voltage-clamp. Glutamatergic and GABAergic currents were distinguished by clamping cells at the estimated reversal for the GABAergic and then the glutamatergic inputs, respectively, and receptive field

maps were generated using synaptic conductances (Fig. 8a; see Methods). The onsets of visually-evoked conductances were defined as the first time point at which the conductance amplitude exceeded 3 times the standard deviation of the noise (see Methods).

We generated estimates of the relative timing of glutamatergic and GABAergic synaptic inputs across receptive fields from a total of 15 control cells. On average, glutamatergic onsets tended to precede GABAergic onsets by a delay of 5.7 ms [95% C.I. = 2.0-8.8], consistent with the presence of a feed-forward circuit[21]. However, there was substantial variety in the delays between the onsets, and there were many regions of the receptive field where GABAergic onset times were synchronous with, or preceded, glutamatergic onsets (Fig. 8b). Some regions only had late glutamatergic onsets, suggesting that the excitatory drive to these regions was entirely polysynaptic. In summary, the whole-cell recordings support a model of the tectum in which the relative timing of glutamatergic and GABAergic synaptic inputs varies across a receptive field, which can help account for the effects of GABAergic signals upon spiking activity and instructive learning.

Discussion

A fundamental idea in developmental neuroscience is that information carried in early activity patterns can guide activity-dependent changes to the functional and structural properties of developing circuits[2,15]. More than simply permitting changes, the spatiotemporal statistics of spiking activity are reflected in the circuit changes that occur[6-10]. Some of the first experimental demonstrations that neural activity plays an instructive role in development involved imposing artificially high levels of correlation between neurons' spiking activity and showing that this disrupted development of receptive field properties in the visual system[4,5]. Later work showed that imposing particular temporal sequences of pre- and postsynaptic spiking activity is able to modify receptive fields in a way that reflects properties of the stimulus[8,10,11]. Here we have extended earlier work describing receptive field changes in the optic tectum[6,11] and have, for the first time, demonstrated that early GABAergic circuits are a key component in this process. Our work suggests that through the spatiotemporal arrangement of glutamatergic and GABAergic inputs, neural circuits may be "wired to learn" from the environment at an early stage.

Axons of retinal ganglion cells in *Xenopus laevis* first innervate the optic tectum at stages 37-39 and GABAergic signals are present soon afterwards[37,30]. Here we show that as tectal cells become visually responsive, these local GABAergic circuits ensure differences in the spatial and temporal spiking patterns of tectal cells. The spatiotemporal correlations in spiking activity between tectal neurons increase when GABAergic circuits are blocked, likely because recurrent excitatory circuits are left unchecked[36], and under these conditions instructive learning is eliminated. Increasing spike-timing correlations between tectal cells during training by electrical stimulation also interfered with learning. These findings are therefore consistent with studies

showing that artificially increasing correlations in activity patterns can disrupt receptive field development[4,5] and reveal that early GABAergic circuits may enhance the tectum's ability to interpret the statistics of the sensory environment and convert these into changes in synaptic inputs. Our findings also suggest that the recurrent excitatory circuitry of the immature optic tectum is normally prevented from dominating plasticity mechanisms, possibly because it has not yet been refined. This is supported by evidence that the temporal precision of recurrent excitation increases at later stages of tectal development[36].

Experimental and computational studies have indicated that STDP mechanisms are able to drive asymmetric changes to excitatory inputs, which could underlie instructive changes in receptive field properties[13,14]. The optic tectum was one of the first places in which a STDP function was described *in vivo*[30] and using these parameters, we showed that GABAergic circuits regulate spiking on a timescale that is relevant for tectal-tectal STDP. Our findings therefore add additional evidence for the importance of STDP in regulating circuit development *in vivo*. One possible discrepancy is the tendency to observe potentiation over depression following training in control cells. Simple extrapolation from spike-pair based STDP would suggest that both potentiation and depression of the receptive field should be seen[11]. However, evidence suggests that the effects of STDP during more complex spiking patterns cannot be fully predicted from a linear summation of the effects of spike-pair based STDP[38]. Also, potentiation may tend to dominate depression under natural conditions of spiking[39]. An important area for future research is therefore to examine how STDP alters circuits under natural conditions.

In mature systems GABAergic circuits can impose precision and synchrony in spiking activity[17-20], and GABA-A receptor blockade often results in an increase in spiking activity and sometimes seizures. In contrast, we observed no significant changes to either spontaneous

activity or the overall activity levels under visual stimulation, suggesting that GABAergic signals in the optic tectum at these stages are not solely inhibitory or excitatory. However, GABA-A receptor blockade did result in a shift in the temporal distribution of stimulus-evoked spike times, such that control cells tended to fire spikes more rapidly but also over a longer period of time. These observations may be related to the relatively depolarizing nature of GABA-A receptor mediated signals at these stages of development[21]. A depolarizing input that can act both as an excitatory drive and/or an inhibitory shunt could produce different effects on spiking activity depending on the timing of the GABAergic inputs relative to the glutamatergic inputs[34,35]. Coupled with our observation that the onsets of glutamatergic and GABAergic inputs vary significantly across individual receptive fields, we can see how GABAergic signals in the immature optic tectum are well placed to increase variability in spike-timing, rather than decrease variance. This also suggests that the effects of GABAergic transmission in the developing tectum are distinct from their effects in mature sensory systems, although there may be interesting parallels to the adult cerebellum[40].

GABA is known to play distinct roles during development that are critical for circuit formation[41], including the modulation of NMDA receptors during synapse formation[21,42,43] and the determination of "critical periods" of heightened plasticity[44]. Our data extend these findings and show that early GABAergic circuits can be fundamental to instructive learning mechanisms. GABA's role in learning appears to be in regulating spike-timing, given that GABA blockade principally altered spike-timing and that other manipulations of spike-timing during the training protocol interfered with learning. However, it should be recognized that GABAergic signals may have other cellular effects that are relevant to learning and which we have not ruled out here. For example, it is possible that under certain conditions GABAergic inputs could also influence

learning by depolarizing tectal neurons to unblock NMDA receptors[21]. Although, the fact that receptive field potentiation occurred at a similar level under GABA blockade and control conditions suggests that this is unlikely to be the primary mechanism.

One might also speculate that the role of GABAergic signals in receptive field changes may alter over the course of development. Evidence from a variety of systems, including the optic tectum, has shown that the balance of glutamatergic and GABAergic inputs changes over the course of development[24], that the receptive field alignment of glutamatergic and GABAergic inputs can change[25], and that there is a shift towards more hyperpolarizing GABA-A receptor activity[28]. It will be interesting to examine whether the potential for instructive learning changes as the GABAergic system, and its relation to the glutamatergic system, matures. In summary, neural systems have evolved to provide animals with an innate perceptual ability but also the ability to adjust their development to the specific features of their environment[3,7,9]. Our work shows that the early wiring of sensory systems may in fact aid this learning from stimulus patterns by enhancing the diversity of neural responses via GABAergic signaling.

Methods

Animals and preparation

All animal procedures were conducted in accordance with UK home office regulations. Wild-type *Xenopus laevis* tadpoles were raised in modified Barth's saline solution, on a 14/10h light/dark at 18°C. Stages of tadpole development were characterized according to established criteria[45] and experiments were conducted between stages 41 and 44. During dissection and electrophysiology, tadpoles were immersed in buffered artificial cerebrospinal fluid (ACSF; in mM: 115 NaCl, 2 KCl, 5 HEPES, 0.01 Glycine, 10 D-Glucose, 3 $CaCl_2$, 1.5 $MgCl_2$, pH 7.2). For the dissection, a 0.01% mixture of the anesthetic tricaine methane sulphonate (MS-222) was added to the ACSF. Animals were pinned upright to a raised platform composed of Sylgard and located in the middle of a custom made image projection chamber (see below). The skin on the head was opened along the dorsal mid-line to expose the optic tectum, and the tectal lobes were separated to expose the ventricular surface. Anesthetic was then washed out via 2 complete exchanges with fresh ACSF. Movement of the animals during recording was prevented with the neuromuscular-junction blocker α-bungarotoxin (3-4 μg/mL; Invitrogen), whose access to the blood stream was aided by a small incision in the animal's tail. All drugs and chemicals were obtained from Sigma unless stated.

Electrophysiology

Patch-clamp recordings were made from the central region of the medial wall of the optic tectum using borosilicate glass micropipettes (4-7 MΩ). The pipettes were filled with an artificial intracellular saline solution (in mM: 110 K-Gluconate, 8 KCl, 5 NaCl, 1.5 $MgCl_2$, 20 HEPES,

0.5 EGTA, 4 Na_2ATP, 0.3 NaGTP, pH 7.2 and osmolarity 250-255 mOsm). Electrical activity was recorded by means of a MultiClamp 700B amplifier controlled by MultiClamp commander software (Molecular Devices). The analog signal was converted to digital at a 10 kHz sampling frequency by means of an analog-to-digital board, and registered by Clampex software version 10.2 (Molecular Devices). Cell-attached recordings were only included if the cell exhibited spiking activity in response to visual stimulation at the end of the recording. Whole-cell recordings were only included if the access resistance remained below 40 MΩ.

For a subset of recordings ACSF containing 50 μM of the GABA-A receptor antagonist SR-95531 (Tocris) was applied locally to the tectum via a glass micropipette by delivering constant air pressure to the back of the pipette. SR-95531 was used because it is considered to be a more selective GABA-A receptor antagonist than other agents[46]. The drug solution was mixed with Alexa Fluorophore 594 (Invitrogen) to allow monitoring of flow (Supplementary Fig. 2a) and data were only included if the drug pipette remained unblocked during the entire recording.

Two other groups of cells were subjected to one of two different manipulations during the training period (see below). In the 'glutamate application' condition, ACSF containing 10 mM L-glutamic acid (Tocris) was puffed locally onto the tectum via a Picospritzer III (General Valve Corporation). Puffs were timed to coincide with the appearance of the training stimuli by using the signal from the photodiode (see below) and puff duration (20-100 ms) was adjusted to maintain spiking activity within the range observed for control cells. In the 'electrical stimulation' condition spiking activity during training was altered via direct electrical stimulation of the rostral optic tectum with a bipolar electrode (Frederick Haer & Co.). For each presentation of the training stimulus, electrical stimulation of the tectum was timed to occur 200 ms following the onset of the visual stimulus. Electrical stimuli consisted of 5 pulses (1 ms duration) at 50 Hz.

The intensity of stimulation was adjusted to ensure reliable spiking activity within the range observed in control cells.

To isolate glutamatergic versus GABAergic currents during whole-cell voltage-clamp recordings, cells were clamped at the estimated GABAergic or glutamatergic reversals, respectively[25,21]. In control cells, reversal potentials for each current were estimated by varying the holding potential between –60 mV and +20 mV while presenting whole-field flashes of light at 0.5 Hz. At a subset of voltages both an inward and an outward current could be seen and the GABAergic reversal was defined as the potential at which the outward current disappeared, while the glutamatergic reversal was taken as the potential at which the inward current disappeared. The reversal of the GABAergic and glutamatergic currents was estimated to be –43.57 ± 1.03 mV and 2.99 ± 0.69 mV (mean ± s.e.m.), respectively. Glutamatergic recordings in SR-95531 were performed at the mean GABAergic reversal estimated from control cells.

Visual stimulation

Recordings were performed with tadpoles positioned in a custom made image projection chamber (Fig. 1a)[47]. One side of the chamber consisted of a semi-transparent wall that functioned as a projection screen and was composed of two glass slides either side of a piece of diffusion filter paper (# 3027 from Rosco Inc.). Visual stimuli were projected through a 12 cm focal length convex lens (Comar) using a computer-controlled LCD projector (Samsung). The maximum luminance of the image projected onto the screen was 13,000 cd/m^2 and the minimum was 22.9 cd/m^2, giving a contrast ratio of 568:1. The projector was attached to a manipulator to allow centering and focusing of the image. In order to time-lock visual stimulation and electrophysiological recordings, the projector also projected onto a photosensitive diode located

below the chamber. The signal from the photodiode was sent to the analog-to-digital board and recorded by the software to produce a signal that could be used off-line to determine onset and offset times of the visual stimuli relative to neural responses with sub-millisecond precision. Visual stimuli were generated by custom made software programmed in C++ using the OpenGL and GLUT libraries. The stimuli covered a square area on the screen of 20 x 20 mm. The animal was placed with its eye located 10 mm away from the screen, so the area of the stimuli corresponded to 90 x 90 degrees of the tadpoles' visual space.

Cell-attached receptive field mapping

To determine how visually driven inputs to tectal cells are altered by experience, a receptive field mapping protocol was utilized before and after the training stimuli were presented (see below). In this protocol the square visual field was divided into an 8 x 8 grid, generating 64 stimulus locations, each comprising 11.25 x 11.25 degrees of visual space. Animals were presented with a series of flashes of white squares on a black background located in one of the 64 locations selected in a pseudo-random order. The flashes occurred at 0.4 Hz. For cell-attached receptive fields, a total of 192 stimuli were presented (i.e. 64 flashes x 3 repetitions = 192 stimuli) producing three repeats for each location in the visual field (Supplementary Fig. 1a). Spikes were analyzed from the first 500 ms following the disappearance of the square from the screen. Individual action potentials in the voltage traces were detected via a threshold (5 times the standard deviation of the noise), which produced spike-rasters containing 3 repeats of the response to each location (Supplementary Fig 1b-c). These spike rasters were then used to estimate the instantaneous rate of fire induced by the flashes. The maximum instantaneous rate of fire was used as the measurement of the strength of inputs from a given location of visual

space, producing a scalar map of the cells' receptive fields. Throughout the manuscript, these measurements are illustrated using heat maps, with the color indicating the response in Hz to flashes in that location of visual space (Supplementary Fig. 1d). Receptive field maps were smoothed using a 2-D Gaussian filter with a standard deviation of 10 visual degrees.

Instantaneous rate of fire was used as the measurement of cells' responses rather than mean rate of fire (the number of spikes divided by the length of time) because it provides information about how a neuron's output evolves over time[48]. Nevertheless, tectal neurons showed a highly significant correlation between maximum instantaneous rate of fire and mean rate of fire (Supplementary Fig. 5a-b, $r = 0.84$, $P = 1.0 \times 10^{-5}$). Moreover, when the receptive fields were measured using mean rate of fire we observed similar effects on receptive fields after training to those we observed using maximum instantaneous rate of fire, both for control condition cells and SR-95531 condition cells (Supplementary Fig. 5c-f). The instantaneous rate of fire was estimated by convolving the spike raster with a Gaussian function with a standard deviation of 10 ms and scaling to produce a continuous measurement in Hz (Supplementary Fig. 1b, top; see ref. 48 for mathematical details).

Receptive field centers were identified as the location in the receptive field map which exhibited the peak response, after smoothing with the Gaussian filter. The receptive field size was considered to be the total area (in visual degrees^2) of visual space that was part of the cell's receptive field. A given location in visual space was considered to be within a cell's receptive field if the mean rate of fire was 2 times greater than the spontaneous mean rate of fire, which was recorded during a 5-60 s epoch.

Assessment of instructive receptive field changes

To determine the effects of visual experience on tectal receptive fields a "training" stimulus was employed that was based on previous work on synaptic plasticity in the optic tectum[6,11]. Training stimuli consisted of a white bar, with a width of 10 degrees, presented on a black background, which moved from one edge of the screen to the other, at a constant rate (90 visual degrees/s). The direction of the movement (the angle of the movement measured counter-clockwise from the horizontal axis) was a randomly selected multiple of 45°. Each presentation of the bar was interposed with 4 s of a black screen. Training lasted for 5 minutes with 60 presentations of the moving bar. To assess receptive field changes in the absence of training stimuli, the screen was set to black for 5 minutes.

To assess the effects of training we generated 'subtraction receptive field maps', which were calculated by subtracting the receptive field map recorded before training from the receptive field map recorded after training, and then dividing by the mean of the pre-training receptive field map (Fig. 1a & 3a). This produced a measure of the percentage change induced by training for each location in visual space. To identify instructive receptive field changes following training three different analyses were employed. First, we measured the change across the subtraction receptive fields in different directions relative to the direction of the training stimuli. In particular, we measured the change across the subtraction receptive fields either in the direction of the training stimulus (e.g. Fig. 2a), or in the direction orthogonal to the direction of the training stimulus (e.g. Fig. 2d). The second method for measuring instructive learning was to calculate an asymmetry coefficient for a given direction. For the asymmetry coefficient in the trained direction the receptive field was divided into two regions along the direction of movement of the training stimulus, and centered on the receptive field centre. For the orthogonal

direction the receptive field was divided perpendicular to the direction of movement of the training stimulus. Therefore, in the case of the trained direction, the two regions represented the receptive field region activated prior to the receptive field center by the training stimuli ('Early') and the receptive field region activated after the receptive field center ('Late') (e.g. Fig. 2b). The asymmetry coefficient was calculated as the scaled difference between the receptive field changes for these two areas (e.g. Fig. 2f). The third method used for assessing instructive changes was to analyze the direction of shifts in the center of receptive fields relative to the direction of movement of the training stimuli. The direction of the shift in the receptive field centers was defined as the angle from the post-training receptive field center to the pre-training receptive field center, measured relative to the horizontal axis of visual space. In cells presented with a blank screen during training the measurements of learning were mimicked by arbitrarily setting the direction of movement of the training stimulus to 0° and performing the same calculations as described above (e.g. Fig. 2e). In a further subset of cells the receptive field mapping protocol was performed twice before training and twice after training (n = 7 control cells, n = 6 SR-95531 cells). These cells were then used to investigate how multi-latency responses (see below) were different before and after training, and the data is provided in Supplementary Figure 6.

Analysis of responses to training stimuli

Recordings were also performed during the presentation of training stimuli. Histograms of the spike-times of each cell during the presentation of the training stimuli were calculated using 10 ms time-bins across the 1s long presentation of the bar (e.g. Fig. 5a). Pair-wise correlations in the

spike-times histograms for each possible pair of cells within a group were calculated, and used to measure the temporal correlations in tectal cell responses during training.

The estimate of STDP potential between tectal cells was based on a Monte-Carlo simulation (Fig. 6j). The Monte-Carlo simulation involved several steps. First, 1000 pairs of cells were randomly sampled with replacement from a given group. For each cell pair, one of the cells was randomly assigned to be the "presynaptic" cell and the other the "postsynaptic" cell (Supplementary Fig. 3). Following this, pairs of spikes were sampled from the cells' actual responses to the training stimuli, in each case taking one "pre-synaptic" spike and one "postsynaptic" spike. A total of 1000 pairs of spikes from the cells' data were sampled with replacement (Supplementary Fig. 3a-c, left). For each pair of spikes, the difference in the timing of the presynaptic spike and postsynaptic spike (Δt) was calculated, producing 1000 values for each pair of cells. A histogram of Δt values was produced, using 1 ms bins (Supplementary Fig. 3a-c, center). These histograms were then weighted by multiplication with a STDP function, $W(\Delta t)$, based on previous work on STDP in the tectum[30,49]: $W(\Delta t) = \{\exp(\Delta t/\tau)$ if $\Delta t < 0$, 0 if $\Delta t = 0$, $-\exp(-\Delta t/\tau)$ if $\Delta t > 0\}$, where $\tau = 15$ ms (Supplementary Fig. 3a-c, right). The STDP estimate was calculated as the absolute value of the sum of the weighted histograms. By taking the absolute value, the STDP estimate could be high regardless of whether LTP or LTD was more likely. This was important because the random allocation of "presynaptic" and "postsynaptic" cells rendered any attempt to distinguish LTP and LTD irrelevant. Thus, the STDP estimate derived from this Monte-Carlo simulation can be thought of as a quantification of the tendency for one cell in a pair to spike before the other within the temporal window necessary for induction of STDP.

Multi-latency receptive field mapping

To measure spiking activity of tectal cells both across visual space and at different post-stimulus latencies we utilized a receptive field mapping protocol that incorporated more repeats. The protocol used the same stimuli described above, but with 1000 flashes presented in a fully randomized order. We measured the mean rate of fire of the cells in a series of 50 ms long time-bins to characterize the temporal evolution of the responses. The higher number of repeats with this mapping protocol improved reproducibility of measurements over these smaller time-windows. A total of 9 different 50 ms time bins were utilized, with the first one starting 50 ms post-stimulus onset and the last one starting 450 ms post-stimulus onset. Therefore the spatiotemporal measurement of a cell's responses consisted of 8 x 8 x 9 data points (64 spatial locations and 9 time bins) and provided an estimate of that cell's preferred stimulus location at each latency (Fig. 7a-b). Correlations in spatiotemporal responses *between* a pair of cells was calculated by treating the entire 8 x 8 x 9 spatiotemporal response map as a vector of length 576, and calculating the correlation coefficient between the vectors. To quantify the correlations *within* a cell's spatiotemporal responses we treated the 3D spatiotemporal data as 9 different vectors each containing 64 locations (Supplementary Fig. 7a). The correlation coefficient for each unique, non-identical pair of these 64 length vectors was calculated, and the average of these 36 unique correlation coefficients was taken as the measurement of spatiotemporal correlation within-cell (Supplementary Fig. 7b).

Whole-cell receptive field mapping

Receptive fields maps measured in voltage-clamp were used to estimate the onset of glutamatergic and GABAergic inputs driven by individual locations of the visual field. Stimulus-

evoked currents were converted into post-synaptic conductances by dividing by the difference between the holding potential and the reversal potential. Each stimulus location was tested once for glutamatergic inputs and once for GABAergic inputs (Fig. 8a) and light-evoked conductances were identified as those with amplitudes that were 3 times the mean amplitude of spontaneous conductances. The onset of a post-synaptic conductance was defined as the first time point at which the trace surpassed 3 times the standard deviation of noise. The delay between light-evoked glutamatergic and GABAergic conductances for each location was then defined as the difference between the GABAergic and glutamatergic onset times (Fig. 8b).

Our measurement of glutamatergic and GABAergic onsets relied on measuring the synaptic conductances at a point at which they were relatively small (9.25 ± 1.13 pA amplitude). This, and the simple morphologies of tectal cells at these stages[50], should reduce the impact of errors associated with voltage-clamp recordings, such as space clamp and series resistance. The fact that glutamatergic conductances recorded under control conditions and during SR-99531 application had similar kinetics (Control rise-time constant = 1.28 ms [95% C.I = 1.11-1.53], SR-95531 rise-time constant = 1.57 ms [95% C.I. = 1.17-2.13], $P = 0.23$, Mann-Whitney *U*-test. Control decay-time constant = 4.63 ms [95% C.I. = 3.31-5.26], SR-95531 decay-time constant = 4.91 ms [95% C.I. = 3.52-7.72], $P = 0.48$, Mann-Whitney *U*-test) and reversal potentials (Control reversal = 4.62 mV [95% C.I. = –0.28-4.64], SR-95531 reversal = 4.64 mV [95% C.I. = 2.17-12.07], $P = 0.19$, Mann-Whitney *U*-test), suggested that measurements of onset were not dramatically affected by the other conductance.

Statistical methods

All data was analyzed using Matlab (Mathworks). Presentation of the data and choice of statistical test depended on whether the data was normally distributed. Normality was assessed using Lilliefors goodness-of-fit test and any data set that produced a significant result at $\alpha = 0.05$ was considered to be non-normal. Normal data are presented in the text and in figures as means ± s.e.m. Non-normal data are presented in the text and in figures as medians with 95% confidence intervals for the medians (as estimated by a bootstrap procedure). Statistical tests of the difference between a group mean and 0 were performed with Student's *t*-test for normal data and a Wilcoxon signed-rank test for non-normal data. Statistical tests of differences between two groups of normal data were performed using Student's *t*-test, while tests between two groups of non-normal data were performed using the Mann-Whitney *U*-test. Tests of differences between multiple groups were carried out with one-way fixed-effects ANOVA tests for normal data, and Kruskal-Wallis one-way ANOVA tests for non-normal data. Pair-wise comparisons between multiple groups were performed using a post-hoc analysis with Bonferroni correction. Tests for correlations in normal data were conducted using Pearson's product moment correlation coefficient, while tests of correlations in non-normal data were done using Spearman's rank correlation coefficient. Tests of differences between distributions were carried out with Kolmogorov-Smirnov tests for all data. All tests were two-sided, and were non-paired unless otherwise stated in the text. Statistical results in the text are given as explicit *P*-values with a lower cutoff of $P = 1.0 \times 10^{-5}$. Statistical results in the figures are presented according to the following convention: n.s. = non-significant (i.e. $P > 0.05$), * = $P < 0.05$, ** = $P < 0.01$, *** = $P < 0.001$.

References

1. Goodman, C. & Shatz, C.J. Developmental mechanisms that generate precise patterns of neuronal connectivity. *Cell* **72**, 77-98 (1993).
2. Katz, L.C. & Shatz, C.J. Synaptic activity and the construction of cortical circuits. *Science* **274**, 1133-1138 (1996).
3. Wiesel, T.N. & Hubel, D.H. Single-cell responses in striate cortex of kittens deprived of vision in one eye. *J. Neurophysiol.* **26**, 1003-1017 (1963).
4. Stryker, M.P. Evidence for a possible role for spontaneous electrical activity in the development of the mammalian visual cortex. in *Problems and Concepts in Developmental Neurophysiology* (ed. Kellaway, P. & Noebels, J.L.) 110-130 (John Hopkins University Press, Baltimore, 1989).
5. Weliky, M. & Katz, L.C. Disruption of orientation tuning in visual cortex by artificially correlated neuronal activity. *Nature* **386**, 680-685 (1997).
6. Engert, F., Tao, H.W., Zhang, L.I. & Poo, M. Moving visual stimuli rapidly induce direction sensitivity of developing tectal neurons. *Nature* **419**, 470-475 (2002).
7. Li, Y., Van Hooser, S.D., Mazurek, M., White, L.E. & Fitzpatrick, D. Experience with moving visual stimuli drives the early development of cortical direction selectivity. *Nature* **456**, 952-956 (2008).
8. Meliza, C.D. & Dan, Y. Receptive-field modification in rat visual cortex induced by paired visual stimulation and single-cell spiking. *Neuron* **49**, 183-189 (2006).
9. Sengpiel, F., Stawinski, P. & Bonhoeffer, T. Influence of experience on orientation maps in cat visual cortex. *Nat. Neurosci.* **2**, 727-732 (1999).
10. Vislay-Meltzer, R.L., Kampff, A.R. & Engert, F. Spatiotemporal specificity of neuronal activity directs the modification of receptive fields in the developing retinotectal system. *Neuron* **50**, 101-114 (2006).
11. Mu, Y. & Poo, M. Spike timing-dependent LTP/LTD mediates visual experience-dependent plasticity in a developing retinotectal system. *Neuron* **50**, 115-125 (2006).
12. Schuett, S., Bonhoeffer, T. & Hübener, M. Pairing-induced changes of orientation maps in cat visual cortex. *Neuron* **32**, 325-337 (2001).
13. Shon, A.P., Rao, R.P.N. & Sejnowski, T.J. Motion detection and prediction through spike-timing dependent plasticity. *Network: Comput. Neural Syst.* **15**, 179 (2004).
14. Wenisch, O., Noll, J. & Hemmen, J. Spontaneously emerging direction selectivity maps in visual cortex through STDP. *Biol. Cybern.* **93**, 239-247 (2005).
15. Weliky, M. Correlated neuronal activityand visual cortical development. *Neuron* **27**, 427-430 (2000).
16. Ramoa, A.S., Paradiso, M.A. & Freeman, R.D. Blockade of intracortical inhibition in kitten striate cortex: effects on receptive field properties and associated loss of ocular dominance plasticity. *Exp. Brain Res.* **73**, 285-296 (1988).
17. Gabernet, L., Jadhav, S.P., Feldman, D.E., Carandini, M. & Scanziani, M. Somatosensory integration controlled by dynamic thalamocortical feed-forward inhibition. *Neuron* **48**, 315-327 (2005).
18. Pouille, F. & Scanziani, M. Enforcement of temporal fidelity in pyramidal cells by somatic feed-forward inhibition. *Science* **293**, 1159-1163 (2001).
19. Wehr, M. & Zador, A.M. Balanced inhibition underlies tuning and sharpens spike timing in auditory cortex. *Nature* **426**, 442-446 (2003).

20. Cobb, S.R., Buhl, E.H., Halasy, K., Paulsen, O. & Somogyi, P. Synchronization of neuronal activity in hippocampus by individual GABAergic interneurons. *Nature* **378**, 75-78 (1995).
21. Akerman, C.J. & Cline, H.T. Depolarizing GABAergic conductances regulate the balance of excitation to inhibition in the developing retinotectal circuit in vivo. *J. Neurosci.* **26**, 5117-5130 (2006).
22. Dunning, D.D., Hoover, C.L., Soltesz, I., Smith, M.A. & O'Dowd, D.K. GABA-A receptor-mediated miniature postsynaptic currents and alpha -subunit expression in developing cortical neurons. *J. Neurophysiol.* **82**, 3286-3297 (1999).
23. Hollrigel, G.S. & Soltesz, I. Slow kinetics of miniature IPSCs during early postnatal development in granule cells of the dentate gyrus. *J. Neurosci.* **17**, 5119-5128 (1997).
24. Liu, Y., Zhang, L.I. & Tao, H.W. Heterosynaptic scaling of developing GABAergic synapses: dependence on glutamatergic input and developmental stage. *J. Neurosci.* **27**, 5301-5312 (2007).
25. Tao, H.W. & Poo, M. Activity-dependent matching of excitatory and inhibitory inputs during refinement of visual receptive fields. *Neuron* **45**, 829-836 (2005).
26. Tyzio, R. et al. The establishment of GABAergic and glutamatergic synapses on CA1 pyramidal neurons is sequential and correlates with the development of the apical dendrite. *J. Neurosci.* **19**, 10372-10382 (1999).
27. Luhmann, H.J. & Prince, D.A. Postnatal maturation of the GABAergic system in rat neocortex. *J. Neurophysiol.* **65**, 247-263 (1991).
28. Mueller, A.L., Taube, J.S. & Schwartzkroin, P.A. Development of hyperpolarizing inhibitory postsynaptic potentials and hyperpolarizing response to gamma-aminobutyric acid in rabbit hippocampus studied in vitro. *J. Neurosci.* **4**, 860-867 (1984).
29. Zhang, L.I., Tao, H.W. & Poo, M. Visual input induces long-term potentiation of developing retinotectal synapses. *Nat. Neurosci.* **3**, 708-715 (2000).
30. Zhang, L.I., Tao, H.W., Holt, C.E., Harris, W.A. & Poo, M. A critical window for cooperation and competition among developing retinotectal synapses. *Nature* **395**, 37-44 (1998).
31. Gao, X. & Van Den Pol, A.N. GABA, not glutamate, a primary transmitter driving action potentials in developing hypothalamic neurons. *J. Neurophysiol.* **85**, 425-434 (2001).
32. Staley, K.J. & Mody, I. Shunting of excitatory input to dentate gyrus granule cells by a depolarizing GABAA receptor-mediated postsynaptic conductance. *J. Neurophysiol.* **68**, 197-212 (1992).
33. Ulrich, D. Differential arithmetic of shunting inhibition for voltage and spike rate in neocortical pyramidal cells. *Eur. J. Neurosci.* **18**, 2159-2165 (2003).
34. Gulledge, A.T. & Stuart, G.J. Excitatory actions of GABA in the cortex. *Neuron* **37**, 299-309 (2003).
35. Chen, G., Trombley, P.Q. & van den Pol, A.N. Excitatory actions of GABA in developing rat hypothalamic neurones. *J. Physiol. (Lond.)* **494**, 451-464 (1996).
36. Pratt, K.G., Dong, W. & Aizenman, C.D. Development and spike timing–dependent plasticity of recurrent excitation in the Xenopus optic tectum. *Nat. Neurosci.* **11**, 467-475 (2008).
37. Holt, C.E. & Harris, W.A. Order in the initial retinotectal map in Xenopus: a new technique for labelling growing nerve fibres. *Nature* **301**, 150-152 (1983).
38. Froemke, R.C. & Dan, Y. Spike-timing-dependent synaptic modification induced by natural spike trains. *Nature* **416**, 433-438 (2002).

39. Sjöström, P.J., Turrigiano, G.G. & Nelson, S.B. Rate, timing, and cooperativity jointly determine cortical synaptic plasticity. *Neuron* **32**, 1149-1164 (2001).
40. Wulff, P. et al. Synaptic inhibition of Purkinje cells mediates consolidation of vestibulo-cerebellar motor learning. *Nat. Neurosci.* **12**, 1042-1049 (2009).
41. Akerman, C.J. & Cline, H.T. Refining the roles of GABAergic signaling during neural circuit formation. *Trends Neurosci.* **30**, 382-389 (2007).
42. Pavlov, I., Riekki, R. & Taira, T. Synergistic action of GABA-A and NMDA receptors in the induction of long-term depression in glutamatergic synapses in the newborn rat hippocampus. *Eur. J. Neurosci.* **20**, 3019-3026 (2004).
43. Wang, D.D. & Kriegstein, A.R. GABA regulates excitatory synapse formation in the neocortex via NMDA receptor activation. *J. Neurosci.* **28**, 5547-5558 (2008).
44. Hensch, T.K. et al. Local GABA circuit control of experience-dependent plasticity in developing visual cortex. *Science* **282**, 1504-1508 (1998).
45. Nieuwkoop, P.D. & Faber, J. *Normal table of Xenopus laevis (Daudin): a systematical and chronological survey of the development from the fertilized egg till the end of metamorphosis*. (North-Holland Pub. Co.: Amsterdam, 1967).
46. Khawaled, R., Bruening-Wright, A., Adelman, J.P. & Maylie, J. Bicuculline block of small-conductance calcium-activated potassium channels. *Pflügers Arch. Eur. J. Phys.* **438**, 314-321 (1999).
47. Niell, C.M. & Smith, S.J. Functional imaging reveals rapid development of visual response properties in the zebrafish tectum. *Neuron* **45**, 941-951 (2005).
48. Dayan, P. & Abbott, L.F. Neural encoding I: firing rates & spike statistics. in *Theoretical Neuroscience: Computational and Mathematical Modeling of Neural Systems* (ed. Sejnowski, T.J. & Poggio, T.) 3-44 (MIT Press, Cambridge, 2003).
49. Song, S., Miller, K.D. & Abbott, L.F. Competitive Hebbian learning through spike-timing-dependent synaptic plasticity. *Nat. Neurosci.* **3**, 919-926 (2000).
50. Tao, H.W., Zhang, L.I., Engert, F. & Poo, M. Emergence of input specificity of LTP during development of retinotectal connections in vivo. *Neuron* **31**, 569-580 (2001).

Figure 1 Examining stimulus-driven receptive field changes in tectal neurons.

(a) Activity of neurons in the optic tectum of *Xenopus laevis* tadpoles was recorded while tadpoles were presented with visual stimuli in a custom built image projection chamber. **(b)** To generate receptive field maps for tectal cells flashes of white squares were presented at different locations of the projection screen and the spiking activity of tectal neurons was monitored by loose-patch cell attached recordings. During training periods a white bar was repeatedly drifted across a black screen in a randomly selected direction, and the spiking activity of tectal cells was recorded. **(c)** Data from a representative cell illustrating the effect of training on its receptive field. To describe the pre-training receptive field a raster plot of the spiking responses to flashes in each area of the visual field was generated and used to calculate the maximum instantaneous rate of fire for each location. These values were then used to generate a colored heat map, as illustrated. The cell was then trained with 60 repetitions of a drifting bar stimulus, during which it responded robustly, as shown in the middle raster plot. Following training, the receptive field was mapped again and exhibited strong differences compared to the pre-training map. To assess the effects of training, the pre-training receptive field was subtracted from the post-training receptive field. The resulting subtraction receptive field shows the percentage change in the maximum rate of fire at each location of visual space.

Figure 2 Moving stimuli instruct asymmetric changes in tectal receptive fields.

(a) Training produced asymmetric changes in receptive fields that reflected the direction of movement of the stimulus. An example cell is shown at the top. Population data (n = 18 cells) is below, showing the mean change in the rate of fire (± s.e.m, shaded region) across visual space, when analyzed in the direction of the training stimulus (arrows). **(b)** Changes around the center of the receptive fields exhibited significant asymmetries. Each pair of points represents the relative change of a cell's receptive field in regions activated by the training stimulus *before* the center ('Early') versus *after* the center ('Late') (**$P < 0.01$, paired *t*-test.). **(c)** The direction of training-induced shifts in receptive field centers (indicated here as Θ) was significantly correlated with the direction of movement of the training stimuli. (Pearson's $r = 0.52$, $P < 0.05$.) **(d)** Receptive field changes in the direction orthogonal to the movement of the training stimuli were symmetric. **(e)** Receptive fields did not show changes in the absence of training stimuli (n = 21 cells). **(f)** Asymmetry coefficients (see Methods) were significantly greater than zero in the direction of training ('Trained'), but not in the direction orthogonal to training ('Orth.'), or for untrained cells at 0° ('Blank'), or for cells that did not spike during training ('No spikes'; n = 2 cells). Data shown is mean ± s.e.m. (*** = $P < 0.001$, n.s. = non-significant, *t*-test.)

Figure 3 Blocking GABAergic inputs eliminates instructive training effects on tectal receptive fields.

(a) Data from a representative cell. In the presence of SR-95531, the training produced changes in receptive fields, but they did not reflect the direction of movement of the training stimuli (conventions as in Fig. 1). **(b)** Receptive field changes analyzed in the direction of the training stimulus (arrows) were not asymmetric. The mean change in the rate of fire (± s.e.m, shaded region) across visual space for a population of tectal neurons trained in the presence of SR-95531 is shown (n = 19 cells; conventions as in Fig. 2a). **(c)** Under GABA-A receptor blockade there was no significant difference in the receptive field regions that the training stimulated before ('Early') and after ('Late') the receptive field centers ($P = 0.5$, paired *t*-test; conventions are the same as in Fig. 2b). **(d)** In the SR-95531 condition, receptive field changes in the direction orthogonal to the movement of the training stimuli were symmetric and resembled those in the direction of the training stimulus. **(e)** Asymmetry coefficients were significantly greater than zero for control cells in the direction of training ('Train. control', same as in Fig. 2f), but under GABA-A receptor blockade the asymmetry coefficients were close to zero for the direction of training ('Train. SR-9'). This was also true for the direction orthogonal to the direction of training ('Orth. SR-9'), and for untrained cells at 0° ('Blank SR-9', n = 7 cells). Data shown is mean ± s.e.m. (**$P < 0.01$, *t*-test).

Figure 4 Effects of GABA-A receptor blockade on baseline receptive field properties. **(a)** Receptive field raster plots from untrained cells illustrating the effect of SR-95531 application upon response properties. Across different receptive field locations a control cell tended to show greater variability in the times of visually-evoked spikes, whereas spikes in a SR-95531 cell tended to occur at similar times following the stimulus and during a relatively short time window. **(b)** Consistent with the examples in (a), there were significant differences in the timing of stimulus-evoked action potentials between control and SR-95531 conditions. Comparing spike-time histograms for all responses of all cells in the two groups it was evident that the onset of responses in SR-95531 cells tended to be later and all spiking occurred over a narrower time window than in control cells. **(c)** Examination of the cumulative distribution functions for these spike-time distributions showed a highly significant difference in spike-timing between the two groups ($P < 0.001$, Kolmogorov-Smirnov test).

Figure 5 GABA blockade boosts temporal correlations between tectal neurons during training. **(a)** As the example cell illustrates (top), control cells fired action potentials at a variety of times during presentation of each drifting bar stimulus and the temporal pattern of spikes differed between cells. This was reflected by the broad shape of the spike-time histogram generated from all responses in control neurons (bottom; n = 18 cells). **(b)** In contrast, the temporal profiles of responses recorded during GABA-A receptor blockade were much more similar across cells. As the example shows, SR-95531 cells exhibited spikes over a relatively short window of time during each presentation of the drifting bar stimulus. This was reflected in the narrow spike-time histogram that was generated from all responses in the SR-95531 population (n = 19 cells), and increased temporal correlations calculated from spike-time histograms of pairs of neurons.

Figure 6 Receptive field changes are altered by manipulations of spike-timing during training. **(a)** Glutamate puffs delivered to the tectum at the start of each presentation of the training stimulus (arrow) increased variability in spike-times (n= 9 cells). **(b)** In the direction of the training stimulus, receptive field changes were no longer asymmetric and showed depression. Data is mean ± s.e.m. **(c)** Changes in the orthogonal direction were similar. **(d)** Direct electrical stimulation of the tectum (arrow) shifted the pattern of spike times so that cells spiked over a narrow time window (n = 11 cells). **(e)** Under these conditions instructive learning was abolished; receptive field changes in the direction of training showed potentiation but no asymmetry. **(f)** A similar profile was seen in the orthogonal direction. **(g)** GABA-A receptor blockade, glutamate puffing and tectal stimulation all abolished asymmetric training-induced changes. Data is mean ± s.e.m, with comparison to 0 via *t*-tests. **(h)** Spikes per presentation of the training stimulus were not significantly different between the conditions. Data is mean ± s.e.m, with one-way ANOVA. **(i)** Compared to control cells, GABA-A receptor blockade and stimulation both caused a significant increase in the temporal correlation between pairs of neurons. Glutamate application decreased temporal correlations. Data is median with 95% C.I. **(j)** Monte-Carlo estimates of STDP between tectal cells revealed that cells in the SR-95531 and stimulation conditions were predicted to have significantly greater potential for STDP. Data is median with 95% C.I. (i) and (j) use Kruskal-Wallis with pair-wise comparisons to controls (* $P < 0.05$, ** $P < 0.01$, *** $P < 0.001$).

Figure 7 GABAergic circuits reduce spatiotemporal correlations in tectal receptive fields. **(a)** Receptive fields were analyzed in the temporal domain by separating responses according to when they occurred after the onset of the flashed stimuli. Data from two representative control cells are shown for seven different time-bins (each 50 ms long) following the onset of the stimuli. As a population, control cells showed greater variety in their responses at different times and different locations of visual space (n = 21 cells). Associated with this variability was the fact that stimuli in some regions of a control cell's receptive field would typically elicit early responses (e.g. 50-100 ms post-stimulus), whereas stimuli in other locations would generate later responses (e.g. 200-250 ms post-stimulus). **(b)** In contrast to control cells, the population of cells recorded under GABA-A receptor blockade showed similar responses at different times and locations of visual space (n = 7 cells). This is illustrated with data from two representative SR-95531 cells here. Maximal responses for the SR-95531 cells occurred between 100-200 ms in post-stimulus time and typically the same receptive field locations elicited both early spikes and later spikes. The result was greater uniformity in the spatiotemporal profile of the responses of different cells in the SR-95531 condition.

Figure 8 The timing of synaptic inputs underlies GABAergic control of tectal spiking. **(a)** Glutamatergic (left) and GABAergic (right) receptive fields were recorded in whole-cell voltage-clamp. The strength of the synaptic inputs to a given location was defined as the integrated conductance of the post-synaptic conductances in the 500 ms following disappearance of the square. The resulting measurements were in units of nS·s, as shown here by the color-coded receptive field maps. **(b)** The onset latencies of glutamatergic and GABAergic inputs were variable across receptive fields. Some locations showed early glutamate followed by GABA (positive delays), some locations showed near synchronous arrival of the two inputs (zero delays) and at other locations GABAergic input preceded glutamatergic input (negative delays). Insets provide example traces showing different delays and population data are from 84 receptive field locations in 15 cells.

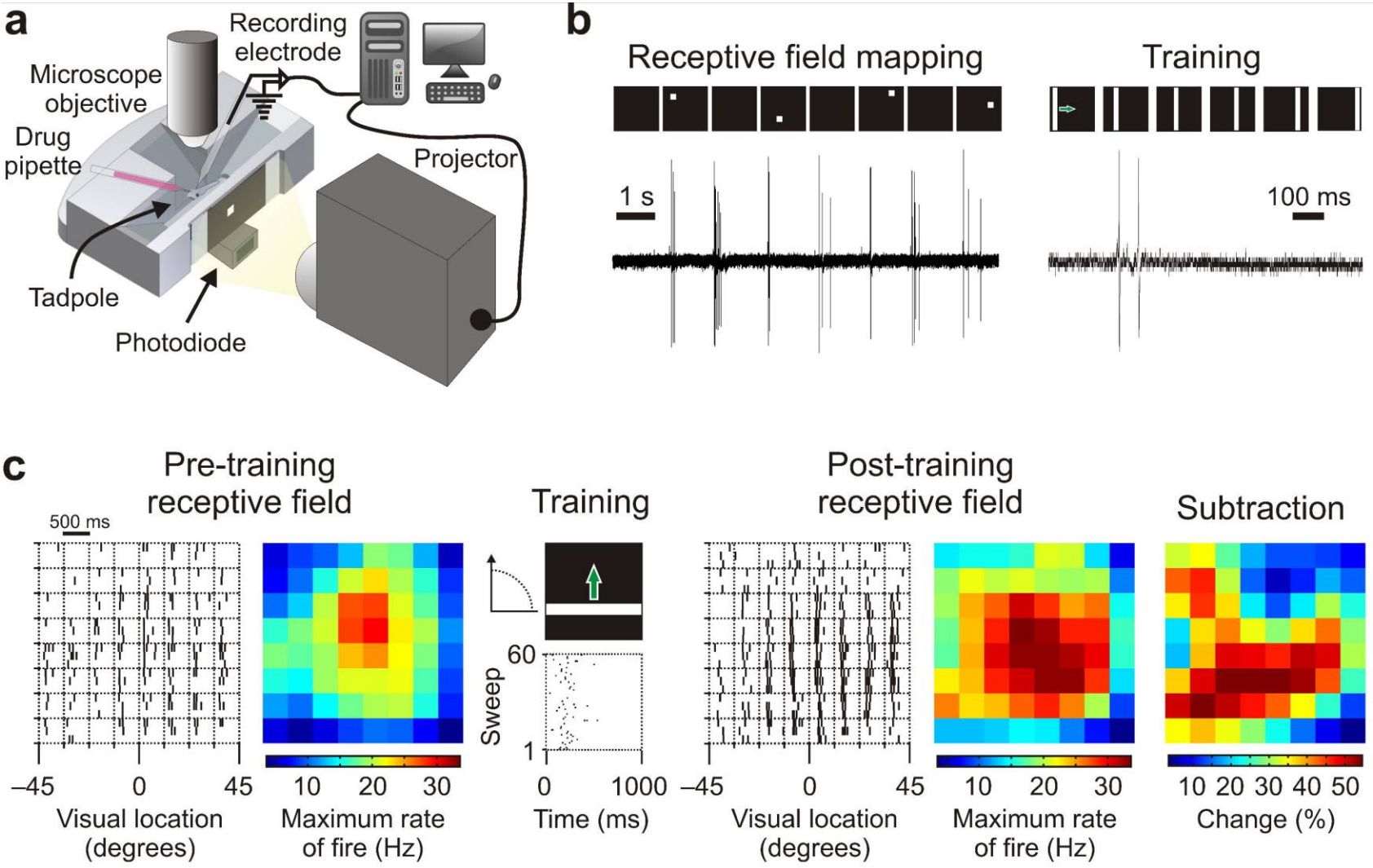

Figure-1 (Akerman)

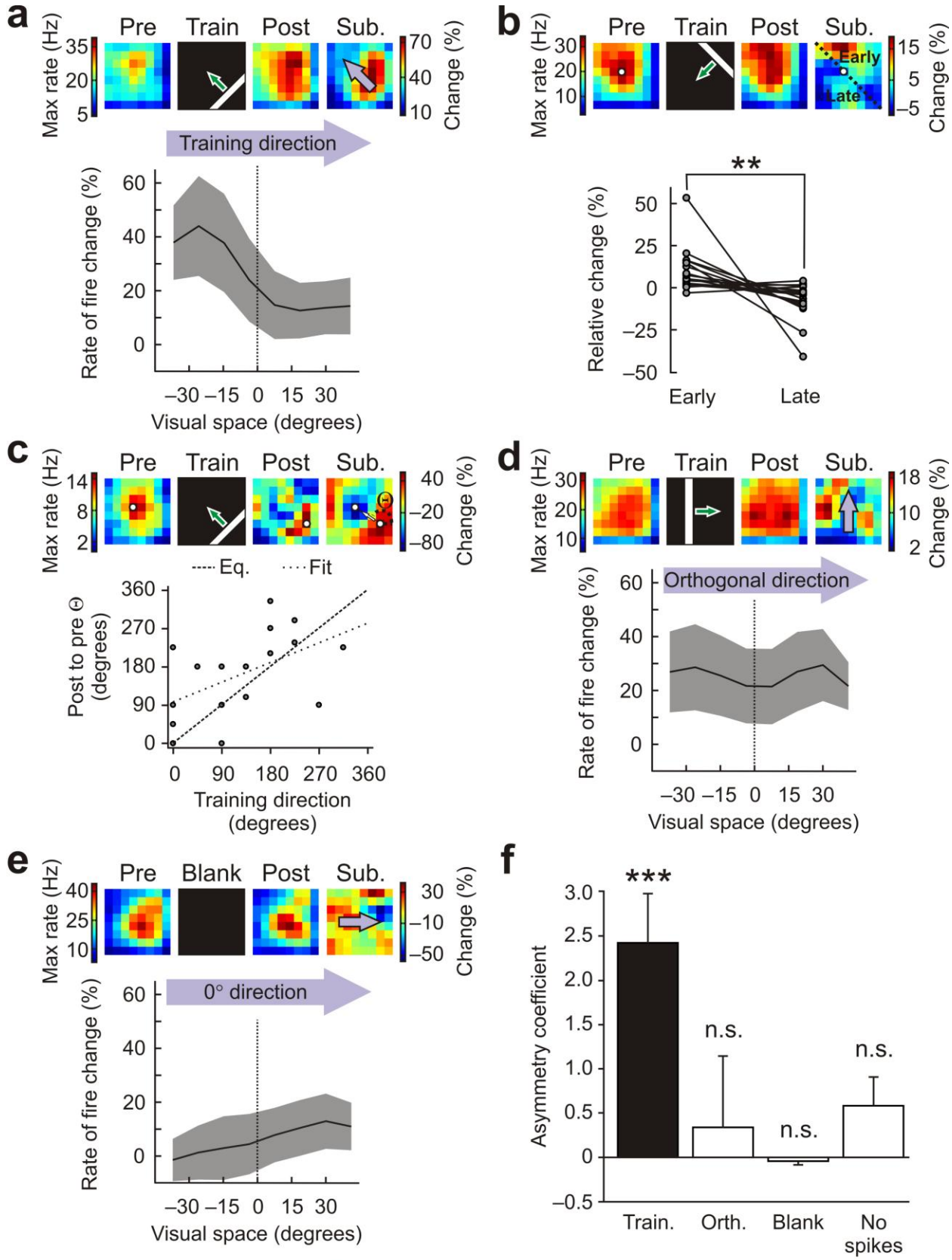

Figure-2 (Akerman)

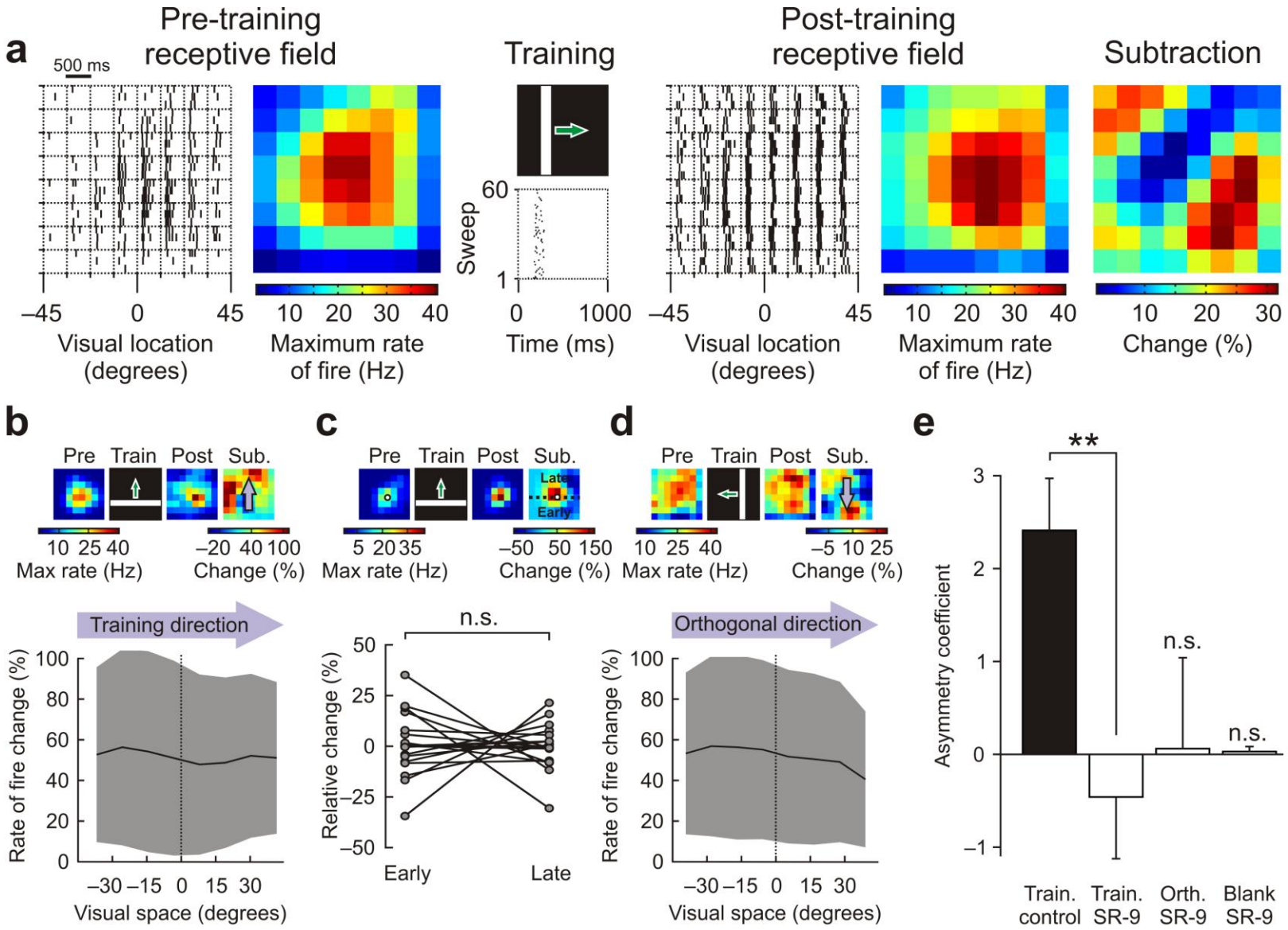

Figure-3 (Akerman)

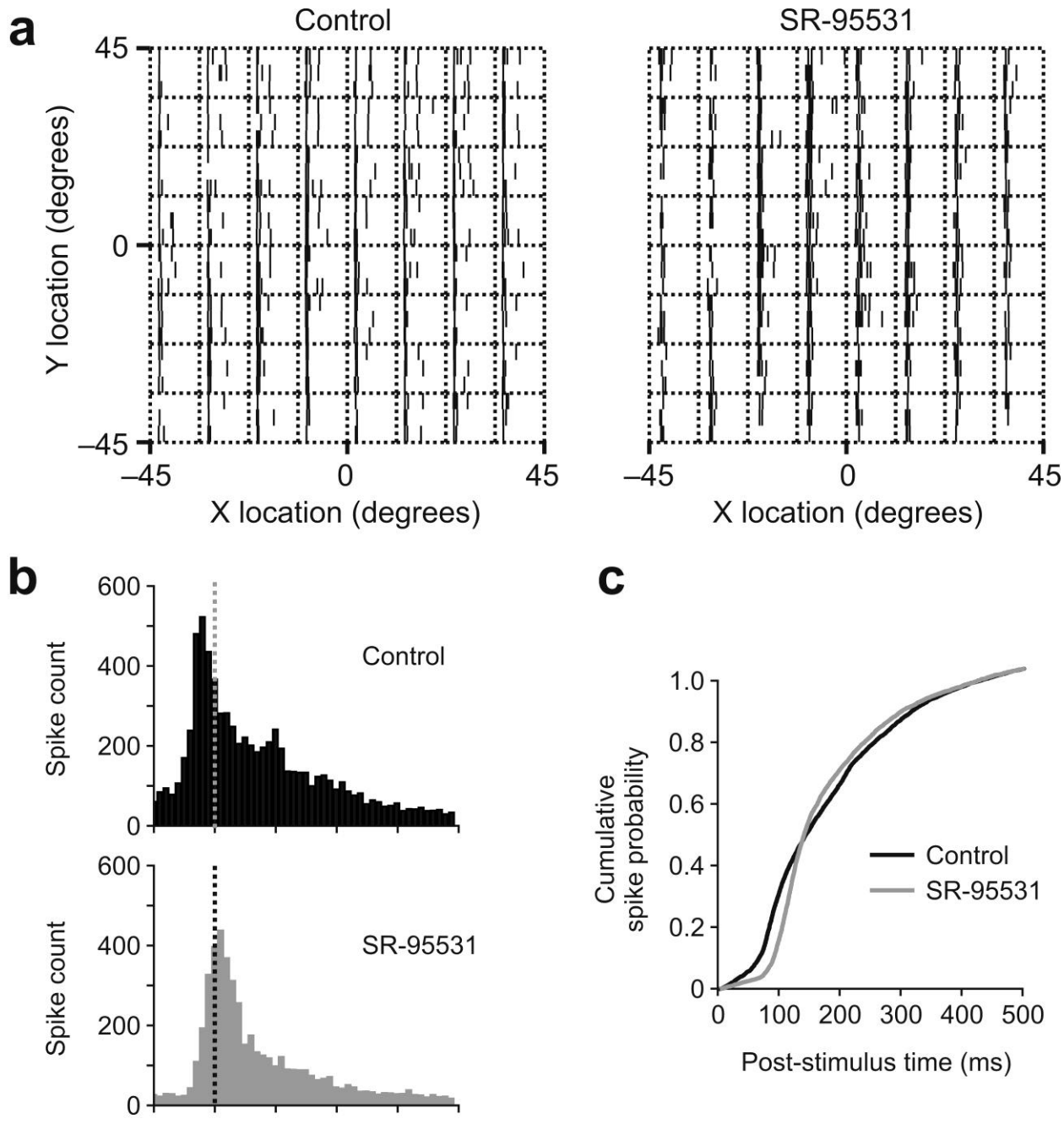

Figure-4 (Akerman)

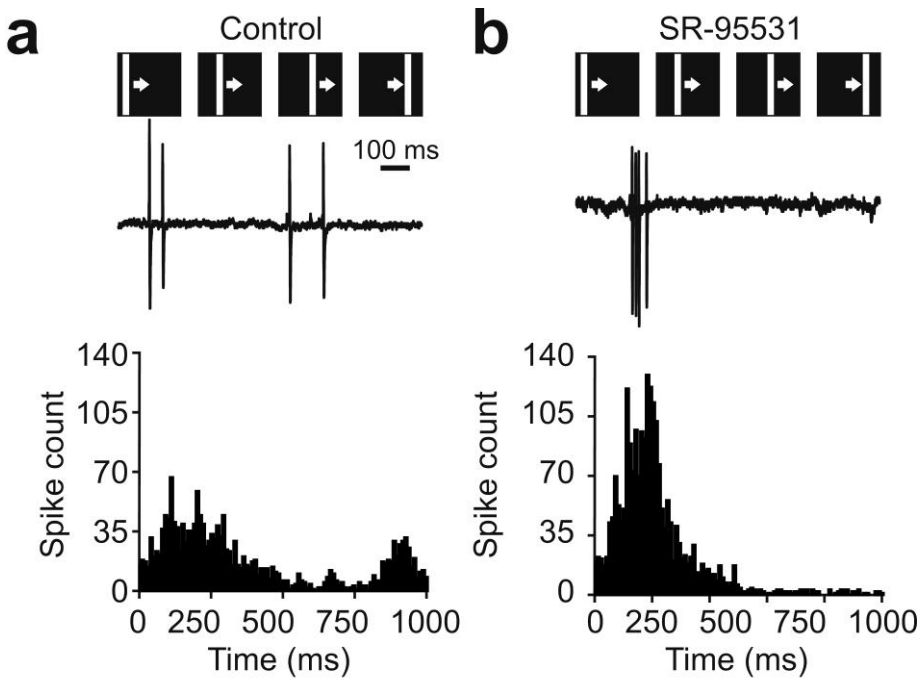

Figure-5 (Akerman)

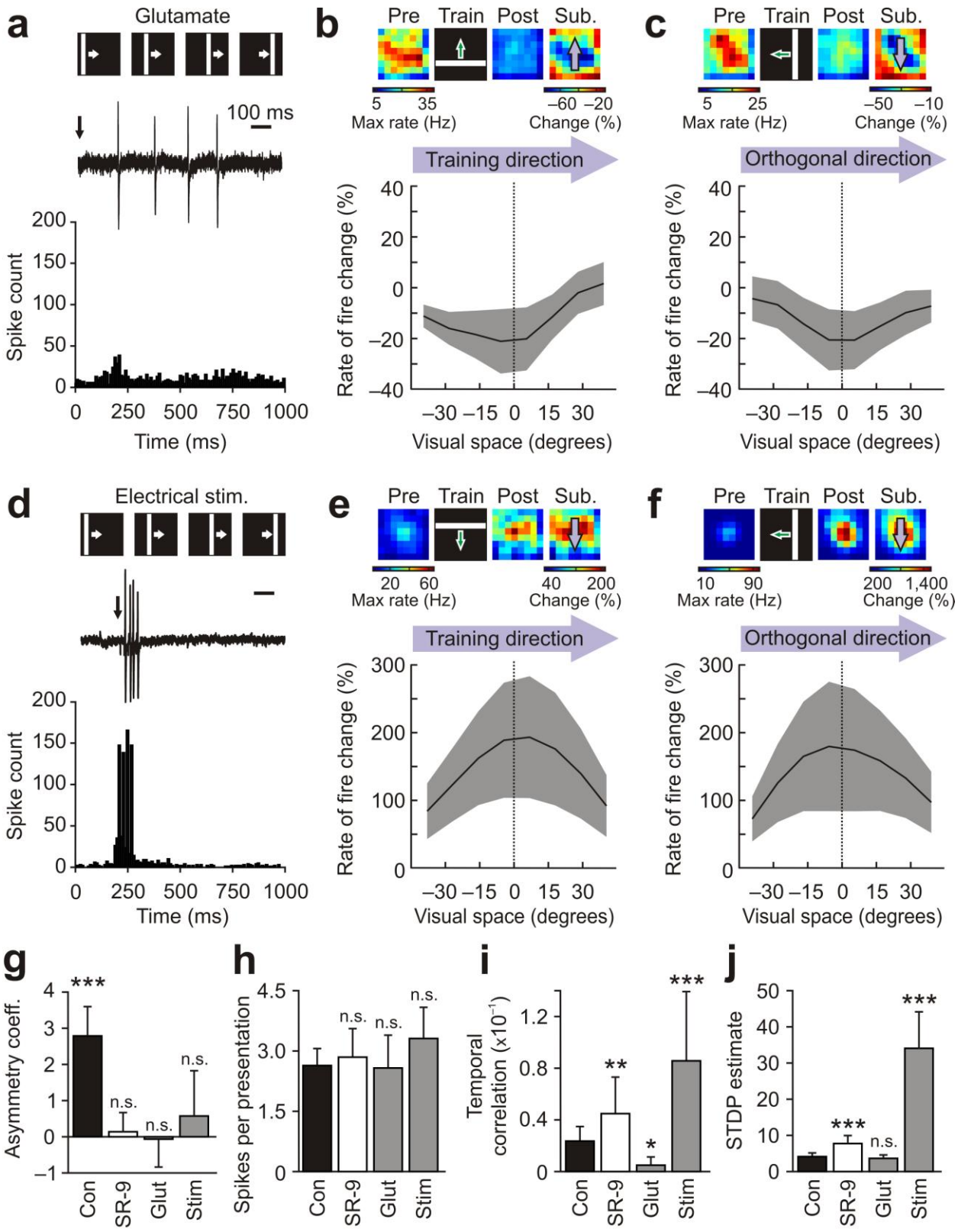

Figure-6 (Akerman)

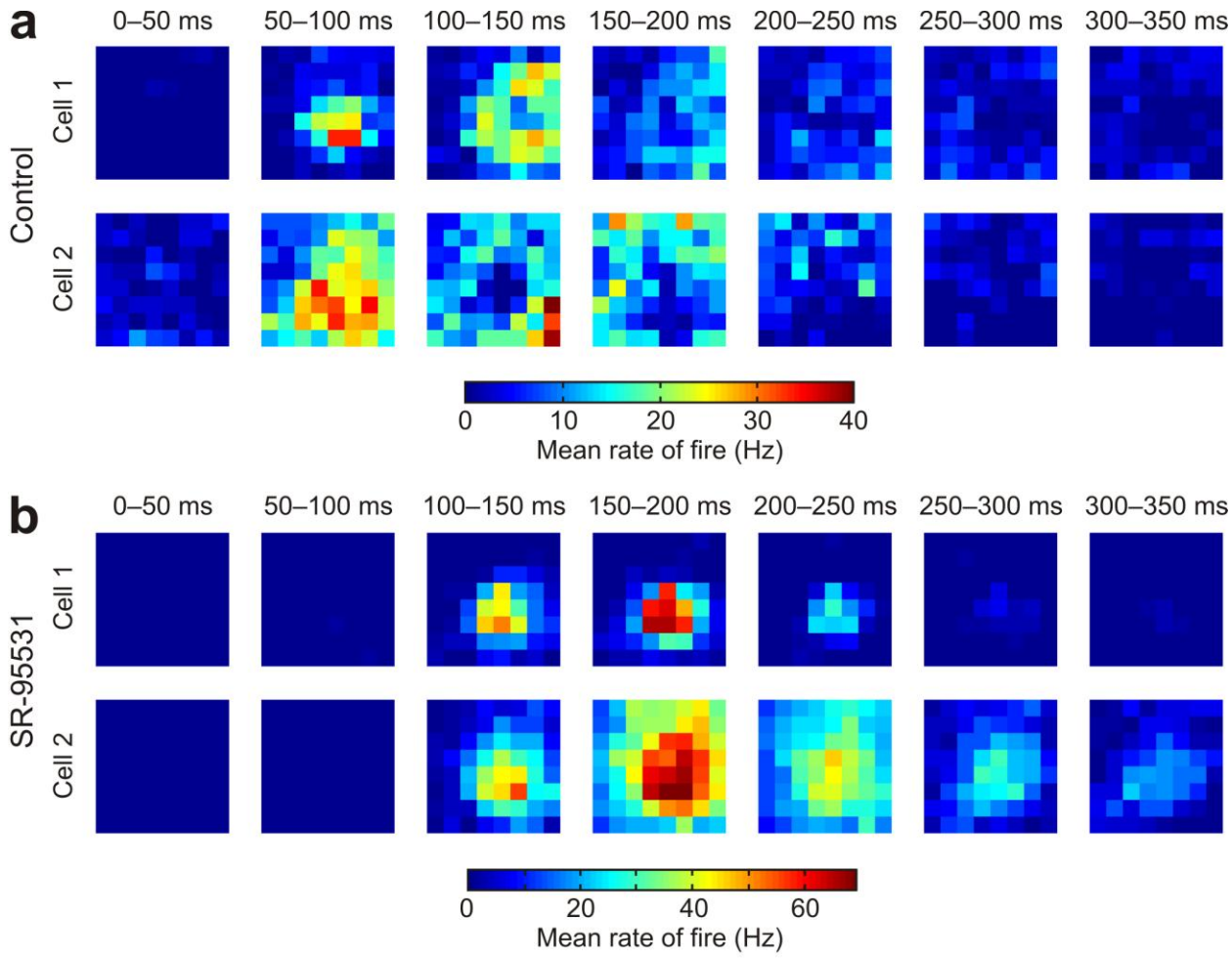

Figure-7 (Akerman)

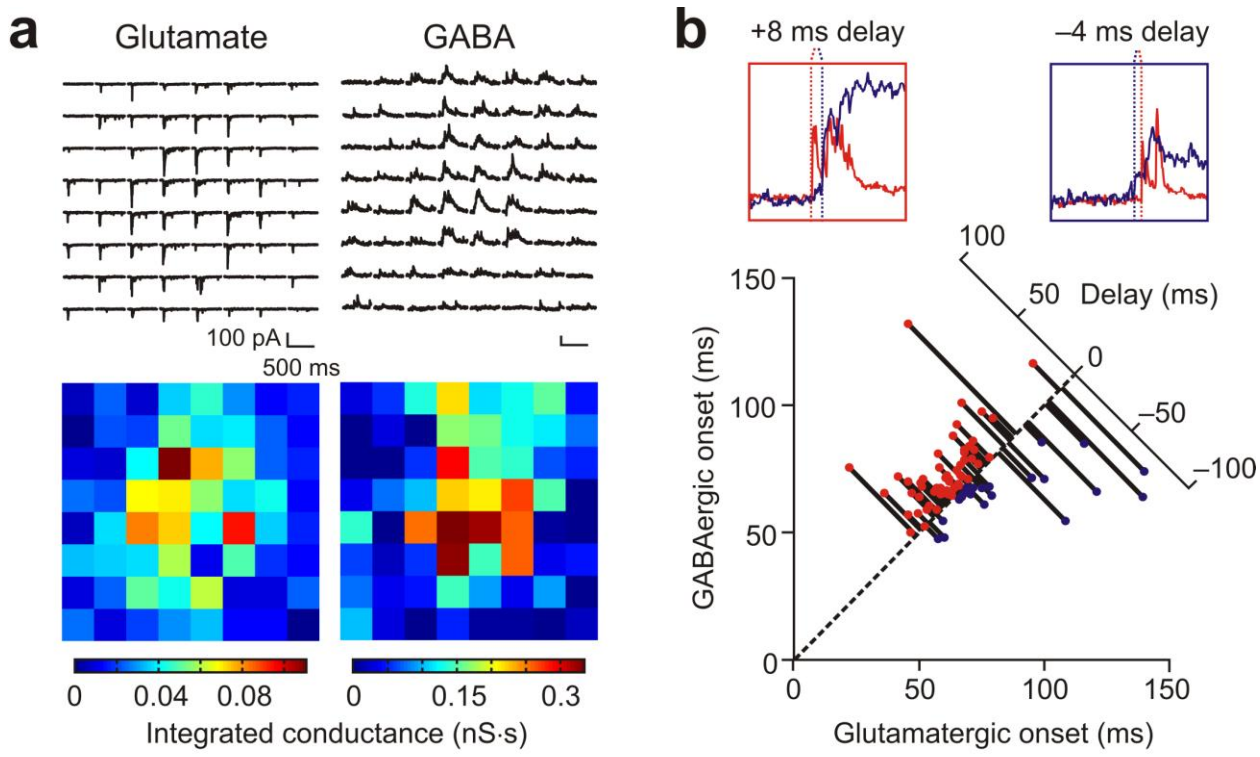

Figure-8 (Akerman)